

See discussions, stats, and author profiles for this publication at: <https://www.researchgate.net/publication/231532502>

# Mixed Chloride/Amine Complexes of Dimolybdenum(II,II). 5. Experimental and Theoretical Study of the Rotation Conformational Preferences of $\text{Mo}_2\text{Cl}_4(\text{R-py})_4$ (R-py = Substituted Pyridin...

ARTICLE in JOURNAL OF THE AMERICAN CHEMICAL SOCIETY · NOVEMBER 1999

Impact Factor: 12.11 · DOI: 10.1021/ja992445x

---

CITATIONS

6

---

READS

9

5 AUTHORS, INCLUDING:



Santiago Herrero

Complutense University of Madrid

43 PUBLICATIONS 425 CITATIONS

SEE PROFILE



Barbara Modec

University of Ljubljana

69 PUBLICATIONS 673 CITATIONS

SEE PROFILE

# Mixed Chloride/Amine Complexes of Dimolybdenum(II,II). 5. Experimental and Theoretical Study of the Rotation Conformational Preferences of $\text{Mo}_2\text{Cl}_4(\text{R-py})_4$ (R-py = Substituted Pyridine) Molecules

F. Albert Cotton,\* Evgeny V. Dikarev, Jiande Gu, Santiago Herrero, and Barbara Modéc

Contribution from the Laboratory for Molecular Structure and Bonding, Department of Chemistry,  
Texas A&M University, P.O. Box 30012, College Station, Texas 77842-3012

Received July 12, 1999

**Abstract:** The relative stabilities of rotation conformational isomers of  $\text{Mo}_2\text{Cl}_4(\text{R-py})_4$  molecules in solution have been studied. R-py represents a substituted pyridine, 4-*tert*-butylpyridine, 4-picoline, or 3,5-lutidine, and the  $\text{MoCl}_2(\text{R-py})_2$  portions of each molecule have the *trans* configuration. In previously reported crystal structures, these molecules have been found with several different conformations:  $D_{2h}$ ,  $D_{2d}$  (both eclipsed), and  $D_2$  (partly staggered). From the visible spectra of these solids, it is found that the  $D_{2h}$  and  $D_{2d}$  conformations give rise to a  $\delta \rightarrow \delta^*$  band at  $\sim 570$  nm, while a  $D_2$  conformation with a twist angle of  $\sim 20^\circ$  from  $D_{2h}$  has a band at  $\sim 645$  nm. For solutions in  $\text{CH}_2\text{Cl}_2$  we find both bands, but the intensity ratio is strongly dependent on temperature. In addition the intensity ratio varies over a range of 100 in THF/ $\text{CH}_2\text{Cl}_2$  mixtures. Calculations by the DFT method provide an estimate of the energy variation as a function of internal rotation angle from the  $D_{2h}$  through  $D_2$  to  $D_{2d}$  conformations. The major conclusions are: (1) the  $D_{2h}$  conformation, although frequently found in crystals, is not stable in solution or the gas phase; (2) the relative stabilities of the  $D_{2d}$  and  $D_2$  conformations vary greatly with solvent and temperature; (3) absorption bands at  $\sim 25\,000\text{ cm}^{-1}$ ,  $20\,000\text{ cm}^{-1}$ , and  $15\,000\text{--}18\,000\text{ cm}^{-1}$  can be assigned to  $\delta \rightarrow d_{x^2-y^2}$ ,  $\pi \rightarrow \delta^*$ , and  $\delta \rightarrow \delta^*$  transitions, respectively.

## Introduction

It was about 35 years ago that the concept of a quadruple bond was introduced to the science of chemistry in order to explain the eclipsed rotational conformation of the  $[\text{Re}_2\text{Cl}_8]^{2-}$  ion. Since that time hundreds of additional compounds containing  $\text{Mo}_2^{4+}$ ,  $\text{W}_2^{4+}$ ,  $\text{Tc}_2^{6+}$ , as well as  $\text{Re}_2^{6+}$  cores have been prepared and characterized.<sup>1</sup> The majority of them have been  $\text{Mo}_2^{4+}$  compounds because of their great ease of preparation and high stability, although the  $\text{Re}_2^{6+}$  complexes are also very numerous.

Rotation about a quadruple bond is governed by the interplay of electronic and steric factors. The principal electronic factor is the  $\delta$  bond energy, and in simple cases, such as the  $[\text{M}_2\text{X}_8]^{n-}$  ions, it is the dominant factor overall. In every case these ions appear to have a  $D_{4h}$  structure, and this is attributed simply (or simplistically?) to the  $\delta$  bonding. In principle, however, it is not clear that attributing this solely to the  $\delta$  bond is rigorously correct. In substituted molecules such as  $\text{M}_2\text{X}_4\text{L}_4$  and  $\text{M}_2\text{X}_5\text{L}_3$  it is certain that interplay of electronic and steric factors is not a simple matter. The sizes and other properties of the substituents, L, and the polarizing of M–X and M–L bonds can have consequences that are not as easily predicted as one might suppose. Finally, we note that practically all experimental information to date concerning rotational preferences has been obtained from crystallographic studies of solid compounds, where intermolecular packing forces can be as large as intramolecular forces. This paper reports the first, and successful, effort to examine the problem in a more direct and fundamental way.

In a recent report,<sup>2</sup> we have shown that molecules of the type  $\text{Mo}_2\text{Cl}_4(\text{R-py})_4$ , where R-py represents an alkyl-substituted pyridine, display rotational conformations about the Mo–Mo quadruple bond that may be  $D_{2h}$ ,  $D_{2d}$ , or  $D_2$ , depending on the crystal in which they are found. These conformations are shown schematically as **I**, **II**, **III** (Scheme 1). In the  $D_2$  molecules the N–Mo–Mo–N rotation angle varies from  $10^\circ$  to  $25^\circ$ . Clearly, whatever inherent conformational preferences the molecules may have, packing forces have a preponderant influence on what actually shows up in a given crystal. Since, as already explained, it is the inherent conformational preference that is of fundamental importance, we have employed theory and solution studies to get insight into this question. However, the spectra of certain of the solids, where the conformations are known by X-ray crystallography, have proved very helpful in confirming our interpretation of the solution spectra. The theoretical work has dealt with the simplest compound, in which R-py is unsubstituted pyridine itself, and the experimental work has focused on the case where R-py is 4-*tert*-butylpyridine because of its high solubility.

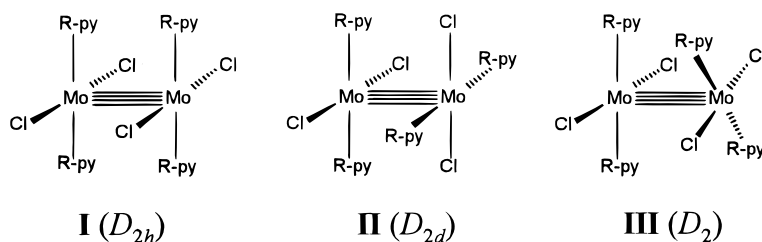
## Experimental and Computational Details

**General Procedures.** All manipulations were carried out under an atmosphere of dry oxygen-free argon or nitrogen with standard Schlenk techniques. Solvents were dried and deoxygenated by refluxing over suitable reagents before use. Deuterated solvents were provided by Cambridge Isotope Laboratories, Inc. Compounds  $\text{Mo}_2\text{Cl}_4(\text{amine})_4$

(1) Cotton, F. A.; Walton, R. A. *Multiple Bonds Between Metal Atoms*, 2nd ed.; Oxford University Press: New York, 1993.

(2) Cotton, F. A.; Dikarev, E. V.; Herrero, S.; Modéc, B. *Inorg. Chem.* **1999**, 38, 4882–4887.

## Scheme 1



(amine = 4-pic,<sup>2</sup> 3,5-lut,<sup>2</sup> 4-Bu<sup>t</sup>-py,<sup>2</sup> NHEt<sub>2</sub>,<sup>3</sup> NH<sub>2</sub>Et,<sup>4</sup> NH<sub>2</sub>Pr<sup>n</sup>,<sup>4</sup> NH<sub>2</sub>-Cy<sup>4</sup>) were synthesized according to published procedures. The new rotamer of Mo<sub>2</sub>Cl<sub>4</sub>(4-Bu<sup>t</sup>-py)<sub>4</sub> was crystallized by cooling to -30 °C a concentrated solution of the compound in acetone.<sup>5</sup>

**Physical Measurements.** Visible spectra of Nujol mulls of the complexes were acquired using a Cary-17D UV-vis spectrophotometer. For the solutions, the HP 853 UV-Visible System was used instead.

**Computational Details.** Theoretical calculations were performed at the density functional theory (B3LYP approach<sup>6-8</sup>) level. Both the standard 3-21G<sup>9</sup> basis set and the valence double- $\zeta$  basis set were used. In the later, a [10s8p5d1f] contraction of the (17s13p8d1f) primitive set by Huzinaga<sup>10</sup> plus two p and one f functions were used for Mo atoms and the valence double- $\zeta$  basis set augmented with d- and p-like polarization functions<sup>9</sup> (6-31G(d,p)) was used for all the ligand atoms. The Gaussian-94 program package<sup>11</sup> was used for the calculations. Geometric structures were fully optimized with the analytic gradient method. Two local minima have been located with both 3-21G and 6-31G(d,p) basis sets. They have  $D_2$  and  $D_{2d}$  symmetric properties, respectively. Some selected geometries of the optimized structure along with the experimental parameters are listed in the Table 1. As expected, the Mo-Mo bond length in the  $D_2$  conformation is slightly longer than that of  $D_{2h}$ . A 23.3° twist in the N-Mo-Mo-N torsion angle weakens the  $\delta$  bond between the metals. The  $D_{2d}$  structure has a lower energy than the  $D_2$ . The energy difference between  $D_2$  and  $D_{2d}$  is calculated to be 4.9 kcal/mol with the large basis set and 3.2 kcal/mol with the small one.

The conformation with  $D_{2h}$  symmetry has been examined in the calculations. It has one zero eigenvalue with both small and larger basis sets. A vibrational frequency analysis at the B3LYP/3-21G level shows there is one and only one imaginary frequency ( $i48.4\text{ cm}^{-1}$ ). This structure is, therefore, to be regarded as a transition state between two equivalent  $D_2$  isomers. The energy barrier amounts to 5.3 kcal·mol<sup>-1</sup> (7.8 kcal·mol<sup>-1</sup> at 3-21G). Since the imaginary frequency is quite small, the energy surface around this transition state must be very flat. Accordingly, the influences from the surroundings might change it into

**Table 1.** Geometries of the Optimized Structure of Mo<sub>2</sub>Cl<sub>4</sub>(py)<sub>4</sub> Compared with Experimental Data Obtained for Mo<sub>2</sub>Cl<sub>4</sub>(4-Bu<sup>t</sup>-py)<sub>4</sub> in the Eclipsed Forms ( $D_{2d}$  and  $D_{2h}$ ) and with a Torsion Angle N-Mo-Mo-N of 25.2°<sup>2</sup>

		$D_{2d}$	$D_2$	$D_{2h}$
Mo-Mo, Å	3-21G	2.113	2.114	2.109
	6-31G(d,p) <sup>a</sup>	2.153	2.156	2.145
	experimental	2.138	2.157	2.140
Mo-N, Å	3-21G	2.249	2.238	2.287
	6-31G(d,p) <sup>a</sup>	2.300	2.288	2.341
	experimental	2.243	2.238	2.243
Mo-Cl, Å	3-21G	2.486	2.486	2.492
	6-31G(d,p) <sup>a</sup>	2.452	2.453	2.456
	experimental	2.415	2.409	2.414
N-Mo-Mo-N, deg.	3-21G	90.0	23.3	0.0
	6-31G(d,p) <sup>a</sup>	90.0	24.2	0.0
	experimental	90.0	25.2	0.0
Cl-Mo-Mo-Cl, deg.	3-21G	90.0	19.0	0.0
	6-31G(d,p) <sup>a</sup>	90.0	19.4	0.0
	experimental	90.0	19.5	0.0

<sup>a</sup> [10s8p5d1f] contraction of the (17s13p8d1f) primitive set by Huzinaga<sup>10</sup> plus two p and one f functions were used for Mo.

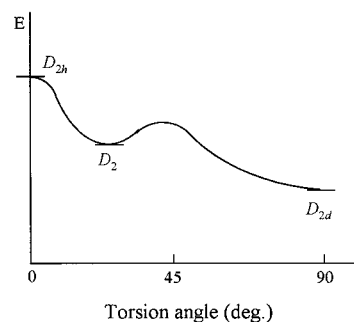


**Figure 1.** Energy of the Mo<sub>2</sub>Cl<sub>4</sub>(py)<sub>4</sub> rotamers vs. N-Mo-Mo-N torsion angle.

a local minimum. An analysis of the vibrational mode for the transition state structure  $D_{2h}$  shows that the mode corresponding to the imaginary frequency is due to the pyridines rotating around their Mo-N bonds. We can visualize a process from the  $D_{2h}$  downhill toward the  $D_2$  structure in which two opposite pyridines rotate in the same direction thus leading to the twisting of the N-Mo-Mo-N torsion angle.

All of the conformations show the typical characteristics of the metal-metal quadruple bonds. The electronic configurations are  $\sigma^2\pi^4\delta^2$  with  $\delta$  as the HOMO and  $\delta^*$  as the LUMO. The energy gaps between the  $\delta$  and  $\delta^*$  orbitals are calculated to be 2.07 eV (2.14 eV with small basis set) for  $D_{2d}$ , 1.85 eV (1.95 eV) for  $D_2$ , and 2.16 eV (2.23 eV) for  $D_{2h}$ .

## Results and Discussion

We begin by considering the results of DFT calculations on Mo<sub>2</sub>Cl<sub>4</sub>(py)<sub>4</sub> (Figure 1). They tell us that in the free molecule, the  $D_{2h}$  conformation is the one least preferred. In fact, it is not even metastable. The first minimum that occurs on rotation away from the  $D_{2h}$  conformation is a  $D_2$  conformation with an N-Mo-Mo-N torsion angle of 23.3°. As rotation continues, there is again a rise in energy followed by descent to a deeper

(3) Cotton, F. A.; Dikarev, E. V.; Herrero, S. *Inorg. Chem.* **1998**, *37*, 5862-5868.

(4) Cotton, F. A.; Dikarev, E. V.; Herrero, S. *Inorg. Chem.* **1999**, *38*, 2649-2654.

(5) Crystal data for  $D_2$ : Mo<sub>2</sub>Cl<sub>4</sub>(4-Bu<sup>t</sup>-py)<sub>4</sub>·(CH<sub>3</sub>)<sub>2</sub>CO: monoclinic, C2/c (No. 15),  $a = 33.092(1)\text{ Å}$ ,  $b = 10.2150(2)\text{ Å}$ ,  $c = 28.944(2)\text{ Å}$ ,  $\beta = 103.282(3)^\circ$ ,  $V = 9522.4(7)\text{ Å}^3$ ,  $Z = 8$ ,  $\rho_{\text{calcd}} = 1.301\text{ g/cm}^3$ ,  $T = 213\text{ K}$ , full-matrix refinement on  $F^2$  (Nonius FAST area detector, SHELXL-93), R1 (on  $F_o$ ) = 0.040, wR2 (on  $F_o^2$ ) = 0.103, GOF = 1.102 for 463 parameters and 54 restraints, 6137 unique data (5619 with  $I > 2\sigma(I)$ ), Mo-Mo 2.1467(5) Å,  $\angle\text{N-Mo-Mo-N} = 19.8(1)^\circ$ . See Supporting Information for other structure details.

(6) Becke, A. D. *J. Chem. Phys.* **1993**, *98*, 5648-5652.

(7) Lee, C.; Yang W.; Parr, R. G. *Phys. Rev.* **1988**, *B37*, 785-789.

(8) Miehlisch, B.; Savin, A.; Stoll, H.; Preuss, H. *Chem. Phys. Lett.* **1989**, *157*, 200-206.

(9) Hehre, W. J.; Radom, L.; Schleyer, P. R.; Pople, J. A. *Ab initio Molecular Orbital Theory*; Wiley: New York, 1986.

(10) Huzinaga, S. *J. Chem. Phys.* **1977**, *66*, 4245.

(11) Frisch, M. J.; Trucks, G. W.; Schlegel, H. B.; Gill, P. M. W.; Johnson, B. G.; Robb, M. A.; Cheeseman, J. R.; Keith, T.; Petersson, G. A.; Montgomery, J. A.; Raghavachari, K.; Al-Laham, M. A.; Zakrzewski, V. G.; Ortiz, J. V.; Foresman, J. B.; Cioslowski, J.; Stefanov, B. B.; Nanayakkara, A.; Challacombe, M.; Peng, C. Y.; Ayala, P. Y.; Chen, W.; Wong, M. W.; Andres, J. L.; Replogle, E. S.; Gomperts, R.; Martin, R. L.; Fox, D. J.; Binkley, J. S.; Defrees, D. J.; Baker, J.; Stewart, J. P.; Head-Gordon, M.; Gonzalez, C.; Pople, J. A. *Gaussian 94*, Revision D.3; Gaussian, Inc.: Pittsburgh, PA, 1995.

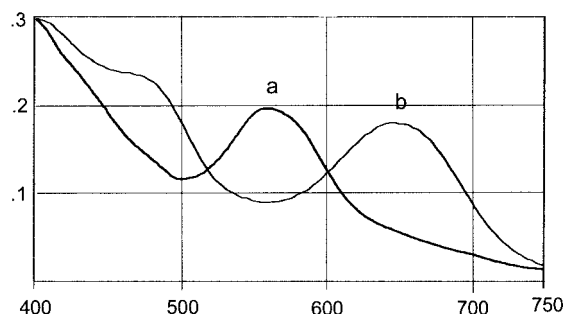


**Figure 2.** Visible spectra of crystalline  $\text{Mo}_2\text{Cl}_4(4\text{-Bu}^t\text{-py})_4$  compounds suspended in Nujol. (a) Cocrystallized eclipsed forms,  $D_{2h}$  and  $D_{2d}$  in ratio 1:2; (b)  $D_2$  with N—Mo—Mo—N torsion angle of  $19.8^\circ$ .

minimum at  $90^\circ$ . The  $D_{2d}$  minimum energy is calculated to be only  $5.3 \text{ kcal}\cdot\text{mol}^{-1}$  below that at  $23.3^\circ$ . Thus, in the gas phase, we should expect the equilibrium constant,  $K$ , at 298 K, to be

$$K = D_2/D_{2d} = 0.00014$$

The entire energy range from  $D_{2h}$  to  $D_{2d}$  is only  $10.2 \text{ kcal}\cdot\text{mol}^{-1}$ , so that the receptivity of the  $\text{Mo}_2\text{Cl}_4(\text{R-py})_4$  molecules to environmental influences is important, in conformity with the previously reported crystallographic results<sup>2</sup> and with the solution results reported here.

Spectra recorded in the region of the  $\delta \rightarrow \delta^*$  transition are shown in Figure 2. It is clear that for the  $D_{2h}$  and the  $D_{2d}$  molecules, in both of which the metal–ligand bonds are eclipsed, the absorption bands are at about 570 nm ( $17.5 \text{ kcal}\cdot\text{mol}^{-1}$ ), whereas for the compound in which the molecule has a  $D_2$  conformation (N—Mo—Mo—N torsion angle of  $19.8^\circ$ ) the band is at 645 nm ( $15.5 \text{ kcal}\cdot\text{mol}^{-1}$ ). This is in reasonable agreement with expectation based on comparison with the known behavior of  $\text{Mo}_2\text{Cl}_4(\text{PR}_3)_4$  compounds.<sup>12</sup>

The results shown in Figure 2 for the specific case of  $\text{Mo}_2\text{Cl}_4(4\text{-Bu}^t\text{-py})_4$  are in accord with a vast amount of literature data (Table 2) for  $\text{Mo}_2\text{X}_4(\text{amine})_4$  molecules in general.

Turning now to a solution of  $\text{Mo}_2\text{Cl}_4(4\text{-Bu}^t\text{-py})_4$  in  $\text{CH}_2\text{Cl}_2$ , let us look at the spectrum at  $20.5^\circ\text{C}$  (Figure 3). There are clearly two overlapping bands in the region 400–700 nm. Curve resolution (after replotting on an energy scale) shows that they are of approximately the same width, with maxima at  $17.5$  and  $15.7 \text{ kcal}\cdot\text{mol}^{-1}$  in a 2.2 to 1 ratio. These can be assigned, respectively, to a conformer which is either  $D_{2d}$  or  $D_{2h}$  and another one,  $D_2$ , with a torsion angle of about  $20^\circ$ ; we estimate this angle based on its position compared with the position from the solid-state visible spectrum of the new rotamer reported here<sup>5</sup> (Table 2 and Figure 2).

As shown in Figure 3, the ratio of the intensities of these two bands is temperature dependent. The isosbestic point for the two bands is consistent with there being only two species present, and thus the upper band is due to either a  $D_{2d}$  or  $D_{2h}$  conformer, but not both. From the theoretical results as well as experimental data to be discussed below, we take this to be the  $D_{2d}$  conformer.

The temperature range accessible is too limited to permit an accurate assessment of  $\Delta H$  for the interconversion, but a value on the order of  $3 \text{ kcal}\cdot\text{mol}^{-1}$  can be inferred. Moreover, since the  $D_{2d}/D_2$  ratio increases with temperature, the  $D_{2d}$  form is less stable than the  $D_2$  form in this solvent. This, of course, is in contrast to the result calculated for the free molecule and shows

**Table 2.** Position of the Absorptions in the Visible Spectra Associated with  $\delta \rightarrow \delta^*$  Transitions (nm) for a Series of Complexes of the Type  $\text{Mo}_2\text{X}_4(\text{amine})_4$

compd	Nujol	THF	$\text{CH}_2\text{Cl}_2$	toluene
$\text{Mo}_2\text{Cl}_4(4\text{-pic})_4$	570 ( $D_{2h}$ ) 580 <sup>a</sup> ( $D_{2d}$ ) 595 <sup>b</sup>	563	567, 640sh	
$\text{Mo}_2\text{Cl}_4(3,5\text{-lut})_4$	555 <sup>a</sup> ( $D_{2h}$ & $D_{2d}$ ) <sup>c</sup> 556 <sup>b</sup>	560, 650sh	570sh, 637	
$\text{Mo}_2\text{Cl}_4(4\text{-Bu}^t\text{-py})_4$	560 <sup>a</sup> ( $D_{2h}$ & $D_{2d}$ ) <sup>d</sup> 645 ( $D_2$ ) 570 <sup>b</sup> 582 <sup>b</sup>	565	565, 640sh	571, 660sh
$\text{Mo}_2\text{Br}_4(4\text{-Bu}^t\text{-py})_4$	603, 661 <sup>b</sup> 665 <sup>b</sup>			
$\text{Mo}_2\text{Cl}_4(\text{NHMe}_2)_4$	555 <sup>e,f</sup>			
$\text{Mo}_2\text{Br}_4(\text{NHMe}_2)_4$	581 <sup>e,f</sup>			
$\text{Mo}_2\text{Cl}_4(\text{NHEt}_2)_4$	547	532	534 <sup>g</sup>	537
$\text{Mo}_2\text{Cl}_4(\text{NH}_2\text{Et})_4$	542	530 <sup>h</sup>	528	529
$\text{Mo}_2\text{Cl}_4(\text{NH}_2\text{Pr}^n)_4$	542	528 <sup>h</sup>	527	530
$\text{Mo}_2\text{Cl}_4(\text{NH}_2\text{Bu}^t)_4$		538 <sup>h</sup>		
$\text{Mo}_2\text{Cl}_4(\text{NH}_2\text{Cy})_4$	529	530 <sup>h</sup>	530	530
$\text{Mo}_2\text{Cl}_4(\text{R-chea})_4$				531 <sup>i</sup>
$\text{Mo}_2\text{Cl}_4(\text{S-chea})_4$				531 <sup>i</sup>

<sup>a</sup> From ref 2. <sup>b</sup> From ref 13. <sup>c</sup> The solid sample contained both kind of crystals. <sup>d</sup> Both isomers cocrystallize. <sup>e</sup> From ref 14. <sup>f</sup> Diffuse reflectance electronic absorption. <sup>g</sup> From ref 3. <sup>h</sup> From ref 4. <sup>i</sup> From ref 15, chea = 1-cyclohexylethylamine.

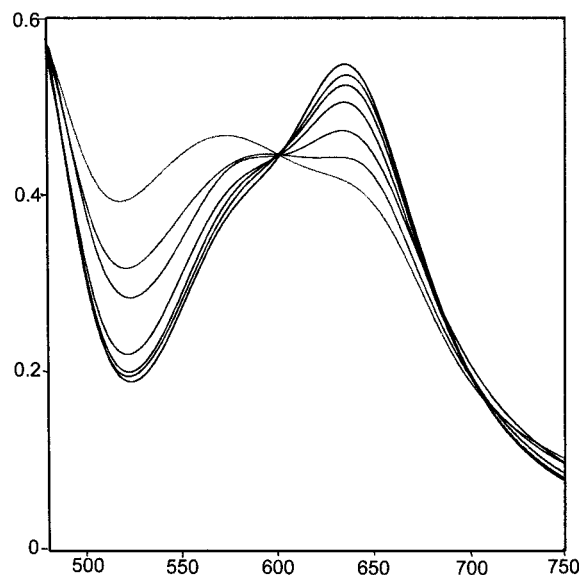


**Figure 3.** Visible spectra of  $\text{Mo}_2\text{Cl}_4(4\text{-Bu}^t\text{-py})_4$  in  $\text{CH}_2\text{Cl}_2$  over temperature range of  $2.5\text{--}29.5^\circ\text{C}$ . Top to bottom at 640 nm:  $2.5, 7.0, 11.5, 16.0, 20.5, 25.0,$  and  $29.5^\circ\text{C}$ .

that solvation effects, like packing effects, profoundly influence the dependence of energy on the angle of internal rotation.

The final, and most informative part of the story depends on the observations reported in Figure 4. This shows that the visible spectrum of  $\text{Mo}_2\text{Cl}_4(4\text{-Bu}^t\text{-py})_4$  depends on the composition of the solvent, for  $\text{CH}_2\text{Cl}_2$ , THF, and mixtures of the two. It is first to be noted, from the behavior of the bands at  $17.6$  and  $16.0 \text{ kcal}\cdot\text{mol}^{-1}$ , that in pure THF the compound is almost entirely in the  $D_{2d}$  conformation, while in pure  $\text{CH}_2\text{Cl}_2$  it is predominantly in the  $D_2$  conformation. Why this should be so is a question to which we have no answer. The dielectric constants of THF and  $\text{CH}_2\text{Cl}_2$  at  $\sim 20^\circ\text{C}$  are not greatly different ( $7.6$  and  $9.08$ , respectively), but, more important, in both conforma-

(12) Campbell, F. L., III; Cotton, F. A.; Powell, G. L. *Inorg. Chem.* **1985**, *24*, 177–181.



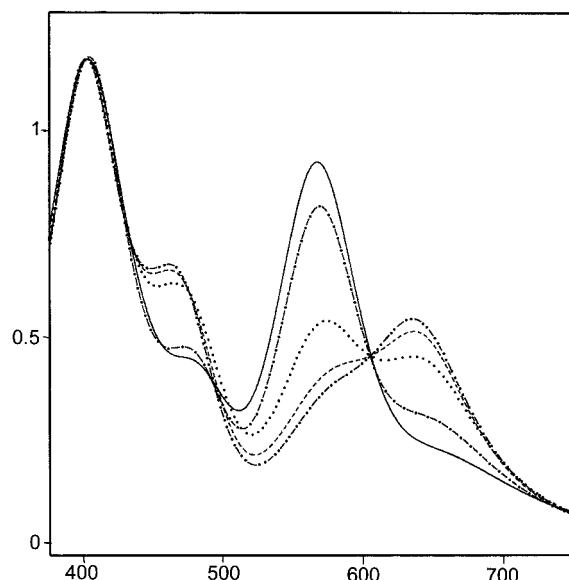


**Figure 4.** Visible spectra of  $\text{Mo}_2\text{Cl}_4(4\text{-Bu}^t\text{-py})_4$  in different THF/ $\text{CH}_2\text{Cl}_2$  ratios at 2.5 °C: 100% THF/THF (—), 70% THF/THF (---), 50% THF (···), 30% THF (— · —), 100%  $\text{CH}_2\text{Cl}_2$  (- · - · - ·).

tions the molecule is nonpolar. We can only assume that owing to solvent–solute complementarities which cannot be explicitly described, THF solvates the  $D_{2d}$  form best.

The idea that THF specifically coordinates in the axial position is negated by the observation that the addition of only one or two equivalents of THF per equivalent of solute in  $\text{CH}_2\text{Cl}_2$  does not cause any change in the spectrum beyond that which would be expected by extrapolation from the rest of the THF/ $\text{CH}_2\text{Cl}_2$  composition range back to a THF/ $\text{CH}_2\text{Cl}_2$  ratio of zero. In addition, it is extremely unlikely that such an axial interaction by THF would differ in strength for the  $D_{2d}$  form compared to the  $D_2$  form.

Another observation which militates against the importance of solvent polarity or axial coordination in determining whether the  $D_{2d}$  or  $D_2$  conformer is preferred is shown in Figure 5. As can be seen, toluene, like THF, favors the  $D_{2d}$  structure, despite the fact that THF is relatively polar and capable of coordination, while toluene is essentially nonpolar and noncoordinating. On the other hand, in acetone, which is the most polar of all the solvents used and also coordinating, the situation is intermediate between that in  $\text{CH}_2\text{Cl}_2$  on one hand and those in toluene or THF on the other.

The next important point about the spectra in Figure 4 concerns the region 380–500 nm. There is a band at  $\sim 25.0 \text{ kcm}^{-1}$  (400 nm) that is essentially constant in intensity even though the intensity ratio of the 17.6 and  $16.0 \text{ kcm}^{-1}$  bands changes by a factor of  $\sim 100$ . Clearly this band is due to a transition that is allowed for both the  $D_{2d}$  and  $D_2$  configurations, and whose energy is approximately independent of the rotation angle in the molecule. At the same time, there is a band at  $\sim 20$

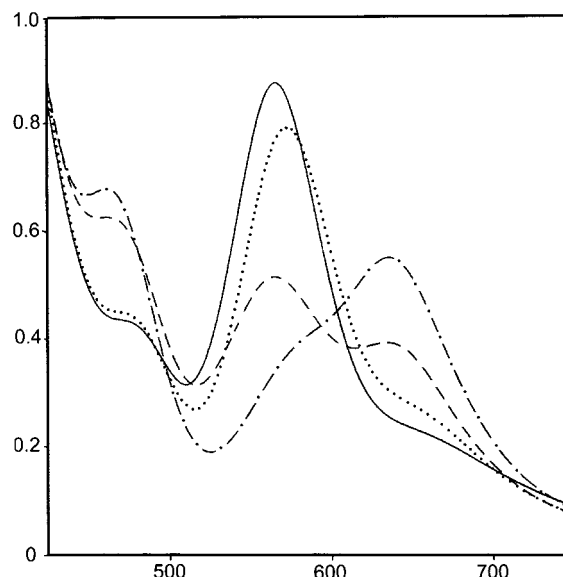


**Figure 5.** Visible spectra of  $\text{Mo}_2\text{Cl}_4(4\text{-Bu}^t\text{-py})_4$  in THF (—), toluene (···), acetone (— · —), and  $\text{CH}_2\text{Cl}_2$  (- · - · - ·) at 2.5 °C.

$\text{kcm}^{-1}$  that is allowed in the  $D_2$  conformation but forbidden in the  $D_{2d}$  conformation.

We shall now show that what is observed in the 380–500 nm range can be fully accounted for. On the basis of the calculations of Norman and Kolari<sup>16</sup> for  $[\text{Mo}_2\text{Cl}_8]^{4-}$  ( $D_{4h}$ ), the only electronic transitions expected at energies below about  $35 \text{ kcm}^{-1}$  are:  $\pi \rightarrow \delta^*$ ,  $\pi \rightarrow \delta^*$ , and  $\delta \rightarrow d_{x^2-y^2}$ . This picture will remain qualitatively unchanged in the  $D_{2d}$  and  $D_2$  forms of the  $\text{Mo}_2\text{Cl}_4(\text{R-py})_4$  molecules, except that the  $\pi$  orbital pair ( $e_u$  in  $D_{4h}$  symmetry) will split slightly into  $b_2$  and  $b_3$  orbitals in  $D_2$  symmetry. Obviously, we already know how to assign the  $\delta \rightarrow \delta^*$  transitions in the  $D_{2d}$  ( $\sim 17.6 \text{ kcm}^{-1}$ ) and  $D_2$  ( $16.0 \text{ kcm}^{-1}$ ) forms of the  $\text{Mo}_2\text{Cl}_4(\text{R-py})_4$  molecules.

A straightforward determination of the allowed or forbidden character of the  $\pi \rightarrow \delta^*$  and  $\delta \rightarrow d_{x^2-y^2}$  transitions gives the following results:

	$D_{4h}$	$D_{2h}$	$D_{2d}$	$D_2$
$\pi \rightarrow \delta^*$	forbidden	forbidden	forbidden	allowed(z)
$\delta \rightarrow d_{x^2-y^2}$	forbidden	forbidden	allowed(x,y)	allowed(x,y)

All experimental results are in accord with these predictions if the  $\pi \rightarrow \delta^*$  and  $\delta \rightarrow d_{x^2-y^2}$  transitions are assigned at 20 and  $25 \text{ kcm}^{-1}$ , respectively, in the  $\text{Mo}_2\text{Cl}_4(\text{R-py})_4$  molecules. Thus, this work provides indirect confirmation for the computational results of Norman and Kolari.<sup>16</sup>

**Acknowledgment.** We are grateful to the National Science Foundation for support of this work. S.H. thanks the Spanish Dirección General de Enseñanza Superior for financial support.

**Supporting Information Available:** Diagrams of molecular orbitals for three rotational isomers (PDF). An X-ray crystallographic file, in CIF format. This material is available free of charge via the Internet at <http://pubs.acs.org>.

JA992445X

(13) Ewing, K. J.; Shupack, S. I. *Polyhedron* **1985**, *4*, 2069–2072.

(14) Armstrong, J. E.; Edwards, D. A.; Maguire, J. J.; Walton, R. A. *Inorg. Chem.* **1979**, *18*, 1172–1174.

(15) Chen, H.-L.; Lee, C.-T.; Chen, C.-T.; Chen, J.-D.; Liou, L.-S.; Wang, J.-C. *J. Chem. Soc., Dalton Trans.* **1998**, 31–35.

(16) Norman, J. G., Jr.; Kolari, H. J. *J. Am. Chem. Soc.* **1975**, *97*, 33–37.